Presentation and experimental validation of a single-band, constant-potential model for self-assembled InAs/GaAs quantum dots

M. Califano and P. Harrison
Institute of Microwaves and Photonics, School of Electronic and Electrical Engineering, University of Leeds, Leeds LS2 9JT, United Kingdom
(Received 27 September 1999)

A single-band, constant-confining-potential model is applied to self-assembled InAs/GaAs pyramidal dots in order to determine their electronic structure. The calculated energy eigenvalues and transition energies agree well with those of more sophisticated treatments which take into account the microscopic effects of the strain distribution on band mixing, confining potentials, and effective masses. The predictions of the model are compared with several spectra reported in the literature by different authors. Very good agreement with both energy position and number of peaks in such spectra is found. The hole energy splitting between ground and first excited states deduced from capacitance and photoluminescence measurements is in excellent agreement with our calculated values. The simplicity and versatility of the model, together with its modest computational demands, make it ideally suited to a routine interpretation and analysis of experimental data.

I. INTRODUCTION

Spatially quantized systems have attracted large interest since the development of molecular-beam epitaxy (MBE) made possible the fabrication of atomically sharp heterojunction interfaces. Recent studies proved three-dimensional (3D) confinement of charge to be attainable within strained islands of many semiconductor heterostructures (SH's) that form on the surface of a substrate during the Stranski-Krastanow[1] growth method. This growth mode proceeds via successive MBE layer depositions of the SH of material 1 on a material 2 SH substrate. Due to the lattice mismatch between deposited material and substrate, after a critical thickness is reached, which depends on the particular heterostructure, the two-dimensional growth changes into a three-dimensional one and coherent[2] (dislocation free) islands of material 1 with a pyramidal shape form spontaneously (with a thin wetting layer left under the islands). The quantum dot (QD) island is then covered (capped) with a layer of the substrate material.

The energy levels of such structures cannot be easily calculated, both because of the finite-potential confining barrier (often of the order of 200–400 meV) and the nontrivial geometry of the dot. The Schrödinger equation must thus be solved by means of a numerical method.

Gershoni *et al.*[3] developed a numerical method in which they expand the envelope function of a rectangular quantum wire (2D confined system) using a complete orthonormal set (COS) of periodic functions, which are solutions for a rectangular wire with an infinite barrier height and suitably chosen dimensions. The advantage of this method is that it can be applied to structures of arbitrary shape. Moreover, all the matrix elements can be calculated analytically. Gangopadhyay and Nag[4] extended this method to study 3D confined structures such as parallelepipeds and cylinders but, to our knowledge such an approach has not been presented so far for pyramidal structures.

The aim of this paper is to extend Gershoni *et al.*'s method to determine the energy levels of pyramidal shaped (self-assembled) InAs dots. In Secs. II and III we give an overview of the method, while Sec. IV presents a critical view of the experimental situation and of the problems connected to the interpretation of the experimental spectra. Finally, in Sec. V we present the results, compare them with the available experimental data, and discuss the method highlighting the most relevant features.

II. THEORY

The Schrödinger equation for the envelope function in the effective mass approximation can be written as

$$-\frac{\hbar^2}{2}\left(\nabla\frac{1}{m^*(x,y,z)}\nabla\right)\Psi(x,y,z)+V(x,y,z)\Psi(x,y,z)=E\Psi(x,y,z). \tag{1}$$

This form ensures, among other things, that it is Hermitian, that the wave functions are orthogonal, and that probability current is conserved at the interface of the heterojunction. The envelope function of the pyramid, $\Psi(x,y,z)$, is then expanded in terms of a COS of solutions of the cuboidal problem with infinite barrier height, i.e.,

$$\Psi(x,y,z)=\sum_{lmn} a_{lmn}\psi_{lmn}(x,y,z), \tag{2}$$

where

$$\psi_{lmn}=\sqrt{\frac{2}{L_x}}\sin\left[l\pi\left(\frac{1}{2}-\frac{x}{L_x}\right)\right]\sqrt{\frac{2}{L_y}}\sin\left(m\pi\frac{y}{L_y}\right)\times\sqrt{\frac{2}{L_z}}\sin\left[n\pi\left(\frac{1}{2}-\frac{z}{L_z}\right)\right]. \tag{3}$$

We have chosen the domains $[-L_x/2,L_x/2]$ and $[-L_z/2,L_z/2]$ for the variation of x and z, and $[0,L_y]$ for that of y (see Fig. 1).

Care has been taken to move the boundaries L_x, L_y, and L_z away from the pyramid, so that the energy eigenvalues are essentially independent of their choice. An attraction of this approach is that there is no need to explicitly match wave

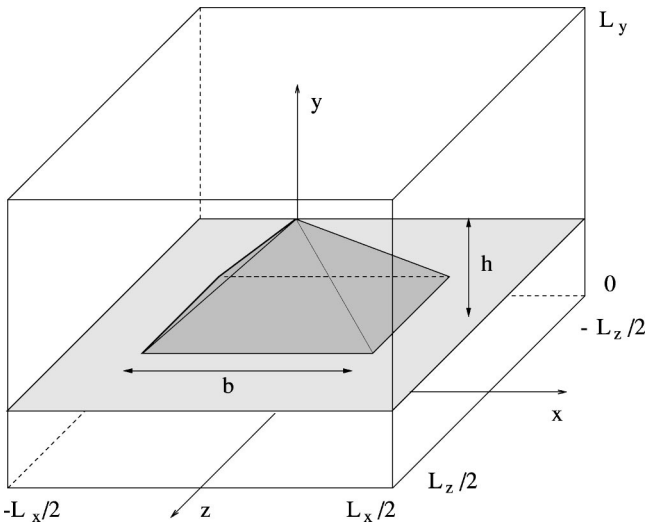

FIG. 1. Schematic representation of the theoretical configuration used in the calculations.

functions across the boundary between the barrier and dot materials. This method is thus easily applicable to an arbitrary confining potential. Substituting expression (2) into Eq. (1), multiplicating on the left by $\psi^*_{l'm'n'}$, and finally integrating over the cuboid $L_xL_yL_z$, yields the matrix equation

$$(M_{mlnm'l'n'} - E\delta_{mm'}\delta_{ll'}\delta_{nn'})a_{lmn} = 0, \tag{4}$$

where use has been made of the orthonormality of the wave functions. The matrix elements $M_{lmnl'm'n'}$ are given by

$$M_{lmnl'm'n'} = -\frac{\hbar^2}{2}\int \psi^*_{l'm'n'}\nabla\left(\frac{1}{m^*(x,y,z)}\nabla\psi_{lmn}\right)dxdydz + \int \psi^*_{l'm'n'}V\psi_{lmn}dxdydz. \tag{5}$$

Carrying out the derivation, the first integral of Eq. (5) becomes

$$-\frac{\hbar^2}{2}\left[\int \psi^*_{l'm'n'}\left(\nabla\frac{1}{m^*(x,y,z)}\right)(\nabla\psi_{lmn})dxdydz + \int \psi^*_{l'm'n'}\frac{1}{m^*(x,y,z)}\nabla(\nabla\psi_{lmn})dxdydz\right]. \tag{6}$$

We then integrate by parts the second integral of Eq. (6): one term (the nonintegral one), coming from the partial integration, vanishes (remember that the wave functions vanish at the boundaries of the cuboid $L_xL_yL_z$), and another term cancels the first integral of Eq. (6), so that we are left with only one term [besides the one containing the potential in Eq. (5)]. We finally obtain

$$M_{lmnl'm'n'} = \frac{\hbar^2}{2}\int \frac{1}{m^*(x,y,z)}\nabla\psi^*_{l'm'n'}\nabla\psi_{lmn}dxdydz + \int \psi^*_{l'm'n'}V\psi_{lmn}dxdydz. \tag{7}$$

The problem here is still the spatial dependence of the effective mass in the integral, i.e., the discontinuity of its value in passing from the well region into the barrier region. To overcome this we split the integral into three parts, within each of which the effective mass is constant: first, we take an integral with $m^* = m_B$ over the whole cuboid (i.e., barrier plus well regions); second, we subtract the integral with $m^* = m_B$ over the well region; and third, we add the integral with $m^* = m_W$ over the well region. The same procedure has been adopted for the integral containing the potential, which is zero in the well region, leading to the final expression

$$M_{lmnl'm'n'} = \left[\frac{\hbar^2\pi^2}{2}\frac{1}{m_B}\left(\frac{ll'}{L_x^2} + \frac{mm'}{L_y^2} + \frac{nn'}{L_z^2}\right) + V\right]\times\delta_{ll'}\delta_{mm'}\delta_{nn'} + \frac{\hbar^2}{2}\left(\frac{1}{m_W} - \frac{1}{m_B}\right)\times\int_W \nabla\psi^*_{l'm'n'}\nabla\psi_{lmn}dxdydz - V\times\int_W \psi^*_{l'm'n'}\psi_{lmn}dxdydz, \tag{8}$$

where the subscript W in the integrals means that the integration is over the pyramidal (well) region. A very relevant feature of this method is that all the integrals in Eq. (8) can be performed analytically. We have used a basis of 19 wave functions in each direction for expanding the envelope function, which is the minimum number required to achieve convergence for the electron energy eigenvalues to within less than 1 meV. Equation (4), where $M_{lmnl'm'n'}$ is a 6859 $\times$6859 matrix, is then solved by using standard mathematical software such as LAPACK.[5]

TABLE I. Calculation parameters: m_B, barrier region effective mass; m_W, well region effective mass (all in units of the bare electron mass m_0); V_0, carrier confining potential (in meV).

Electron			Heavy hole					
			Parametrization C			Parametrization G		
m_B	m_W	V_0	m_B	m_W	V_0	m_B	m_W	V_0
0.0665	0.040	450	0.3774	0.59	266	0.3774	0.341	316

III. MODEL AND ITS APPLICATION

Energy levels of pyramidal shaped InAs/GaAs dots have been calculated using the parameters values listed in Table. I. In the dot material the compressive stress alters the curvature of the bulk bands, causing the effective masses to differ from the unstrained ones. We have used the value of $0.04m_0$ (Ref. 6) for the effective mass of InAs in the conduction band (the unstrained value is $0.023m_0$) to account for the strain, as suggested by Cusack *et al.*[7] Most authors use two different values for the hole effective masses, one along the symmetry axis z and the other along the plane xy normal to that axis, to account for the mass anisotropy. This choice while on one hand increasing the (computational) complexity of the treatment, on the other hardly improves the approximation, the mass for the motion along transverse directions (where the holes spend the most of their time) still being undefined. Accurate pseudopotential calculations in quantum wells[8]

have revealed the in-plane masses m_{xy}, of electrons, light holes, and heavy holes to be similar to those commonly accepted for the motion along the z axis. The values for the heavy-holes effective masses in InAs along the [001] and [111] directions, i.e., $m_{hh,z}$ and $m_{hh,xy}$, used by Grundmann *et al.*[9] in their calculations, differ by only 2.5%, whereas Cusack *et al.*[10] predicted very different values: $m_{hh,z}=0.590$ and $m_{hh,xy}=1.347$. In the latter work, however, the difference for the light-hole effective masses along the growth and the in-plane directions is only about 7%. Aiming at a realization of a simple (but not necessarily less reliable or less accurate) model, every unnecessary complication which, after confirmation, does not significantly improve the agreement with experiment or introduce additional physical effects, has been avoided. We therefore restricted ourselves to only one value for the hole effective mass, i.e., $m_{hh}=m_{hh,z}$.

Performing empirical pseudopotential and *ab initio* local-density calculations for the band structure of InAs under strain, Cusack *et al.*[10] estimated the mass for the heavy holes along the [001] (z) direction to be $0.590m_e$, near the center of the pyramid in structures with an aspect ratio of 1. On the other hand, Grundmann *et al.*[9] used a value of $m_{hh,z}=0.341$ in their calculations, also for pyramids with an aspect ratio of 1. We performed our calculations using both, aiming to decide after comparison with experimental results which one was better suited for describing the system. For the heavy-hole effective mass in the barrier (GaAs) material, the commonly accepted value of $m_{B,hh}=0.3774$ has been taken.

The strain affects the confining potential of the carriers as well, which becomes a piecewise continuous function of position,[7] and differs from the square well formed by the difference in the absolute energy of the conduction- or valence-band edges in the bulk dot and barrier material. The square well (constant potential) approximation, however, still gives good results for the conduction band;[9] thus the electron confinement potential has been taken as the average over the QD, i.e., $V_0=450$ meV.[9] Even though the same treatment is less suitable for the hole's confining potentials, their shapes being more complex, we assumed them to be constant within the dot. The average heavy-hole confining potential relative to each of the mass values has been determined by performing several calculation sets, for all dot dimensions considered, with different values of $V_{0,hh}$, and choosing the potential value which gave the best agreement with the theoretical results reported in the cited papers. We therefore determined two different parametrizations (i.e., two different pairs $V_{0,hh}$ and $m_{hh,z}$), for the heavy holes (see Table I): *C* (after Cusack *et al.*, the results of which are well reproduced by this set of values) and *G* (for Grundmann *et al.*, this set giving the best agreement with their calculations).

The strain also induces a piezoelectric polarization, which results in a piezoelectric potential $V_p(x,y,z)$. However it generally affects the energies of levels involved in optical transitions by less than 1 meV;[9] therefore, it has been disregarded in our calculations. The inclusion of such a potential would reduce the symmetry of the pyramidal dot from C_{4v} to C_{2v}, leading to a lifting of degeneracies. The Coulomb interaction has also been neglected since the QD's considered are in the *strong confinement regime*,[11] the size quantization representing the main part of the carrier energy (their effective radius is small compared to the bulk exciton Bohr radius).

TABLE II. Dimensions of the structures studied.

Structure	b(Å)	h(Å)
1	60	30
2	80	40
3	100	50
4	120	60
5	140	70
6	160	80
7	180	90
8	200	100

Since it has been reported[9] that the strain distribution in a quantum dot does not depend on the actual *size* of the dot but on its *shape*, (provided that the aspect ratio of half base and height also remains constant[10]), the same values for effective masses and potential have been used throughout the calculation for all the dot sizes considered (see Table II).

IV. EXPERIMENTS AND THEORETICAL CALCULATIONS

A huge quantity of experimental data are available on InAs/GaAs QD's since the fabrication of samples with narrow size and uniform density distribution has been made easy to achieve by the Stranski-Krastanov growth method.[1] Islands of various sizes and shapes have been reported, depending on the growth conditions, such as temperature, InAs coverage, growth rate, time delay before GaAs regrowth, etc. The dots grown by Grundmann *et al.*[12] have been observed to be square-based pyramids by high-resolution transmission electron microscopy, whereas the same shape for the dots studied by Moison *et al.*[14] has been evidenced by atomic force microscopy (AFM) images. Fricke *et al.*[15] and Leonard *et al.*[13] estimated their InAs islands to be lens shaped from atomic force micrographs. Finally, Sauvage *et al.*[16] reported the dots investigated in their work to have a square base pyramidal shape before GaAs regrowth, and a lens shape after that, with a smaller size than what is observed by AFM, due to the quenching of their evolution by the GaAs deposit. The effect of capping could result on another hand in a slight elongation of the dots as a reminder of the extreme anisotropy of InAs islands on GaAs for submonolayer coverage, as suggested by Nabetani *et al.*[17] and Fricke *et al.*,[15] who reported experimental evidence (far-infrared FIR spectra) about the associated breaking of the symmetry in the first and second excited electron states.

The tools employed to investigate the size and shape of these islands can be divided into two groups: On the one hand there are techniques such as scanning tunneling microscopy and AFM which allow the dots to be seen directly but need them to be uncapped, whereas the samples used in the actual measurements [of photoluminescence (PL) spectra, for instance] are all capped (the usual way to proceed is to grow two samples in the same conditions and to cap one of them for the measurements, leaving the other uncapped for the

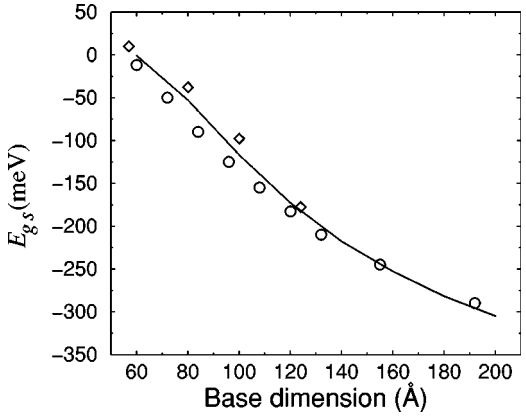

FIG. 2. Electronic energy levels as a function of base length, for InAs square-based pyramidal QD's, with respect to the unstrained GaAs conduction band. Comparison of our results (full line) with those of Ref. 7 (diamonds) and Ref. 9 (circles).

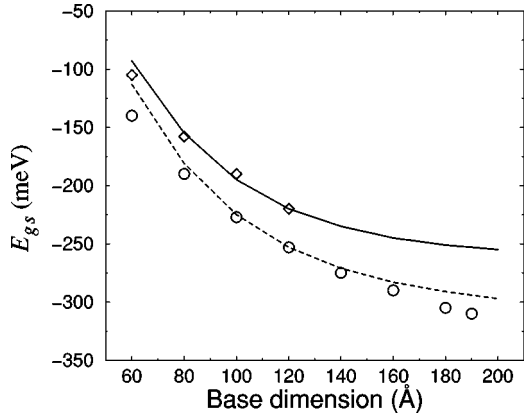

FIG. 3. Heavy-hole energy levels as a function of base length, for InAs square-based pyramidal QD's, with respect to the unstrained GaAs valence band. Comparison of our results [full (parametrization C) and dashed (parametrization G) lines] with those of Ref. 7 (diamonds) and Ref. 9 (circles).

AFM investigations. As it is clear from the preceding discussion however, the capping process may introduce both shape and size variations in the islands). On the other hand, analysis such as TEM can give structural information on capped QD's, but the images tend to overestimate the dot's dimensions and do not give good estimates of the composition. Another structural investigation technique, scanning transmission electron microscopy, was recently proposed,[18] which allows more detailed estimates of the size and shape of the dots to be made, avoiding the problems associated with the usual TEM.

An accurate estimate of size and shape of the islands emitting a given PL spectrum (which is essential for theoretical calculations to give an accurate description of the electronic structure of the QD, and therefore to succesfully reproduce its spectral features), is nevertheless still very difficult to obtain. Moreover the situation for the theorist is made even more complex by the shape of the PL spectra: due to the size distribution of the dots in the sample, in the best cases they have a full width at half maximum (FWHM) of about 50 meV, which is too broad an energy range to represent a severe enough test for a theoretical model.

So far we have considered only the main feature of the PL spectra, where the strong signal is attributed to recombination from the dot ground state. The origin of higher-energy spectral features is still the subject of some debate at the present time. Grundmann *et al.*[9] attributed them to transitions between the electronic ground state and several hole states, allowed by the lack of symmetry along the growth axis, whereas Schmidt *et al.*[19] identified them with transitions between states with the same quantum numbers.

Aware of all these limitations we have tried to apply our simple model to interpret the experimental features of several PL spectra, not pretending to be able to reproduce them in great detail, but aiming at putting our theory to the test, in order to determine its range of applicability and its potentiality. In Sec. V we compare our predictions with those of two other different theoretical approaches as well.

V. RESULTS AND DISCUSSION

In Fig. 2 we present the results for the InAs QD electron energy levels as a function of the base dimension, plotted relative to the unstrained GaAs conduction-band edge, and compare them with the results of Refs. 7 and 9. Despite the simplicity of our calculations, which do not account for band mixing and the spatial variation of the confining potentials due to strain, but assume a constant average (strained) potential throughout the dot, the ground-state electronic energies given by our method agree very well with those, more sophisticated, theoretical studies which take into account all these features.

Our model predicts no bound electron states for base lengths smaller than about 60 Å, and three electron levels for structures with base dimensions between approximately 120 and 160 Å. This number increases for bases larger than 160 Å, up to ten bound states for 200 Å. As in Ref. 7, the first and second excited electron states have been found to be degenerate, as expected, due to the C_{4v} symmetry of the pyramidal dot.

By choosing two different couples (C and G in Tables I and IV) of well effective masses and average confining potentials, the heavy-hole ground-state eigenenergies obtained in the previously cited references have been reproduced (see Fig. 3), and the calculated energies for the $C1 \rightarrow V1$ transition in each structure consequently agree well with those values.

In Ref. 20, Grundmann *et al.* compared the results of their calculations with experimental PL data. Their model predicts only one bound electron state, therefore the peaks are attributed to transitions between the ground-state electron level and ground or excited hole states. Unfortunately Grundmann *et al.* did not give the exact dimensions of the QD the PL spectrum refers to. They referenced a previous paper of theirs, but there they presented the absorption spectrum of a sample with average deposited InAs thickness $t_{av}=1.2$ nm, (base 12 ± 1 nm, height 5 ± 1 nm), whereas the PL spectrum of Ref. 20 refers to a $t_{av}=1.0$ nm sample. We have deduced the approximate dimensions of the dot by comparing the values they presented in the diagram for the transition energies as a function of pyramid size and the values they reported on the PL spectrum as their predicted transition energies. In Table III we report the energetic positions of the PL peaks together with our theoretical predictions for a

TABLE III. Transition energies: comparison between experimental values (deduced from PL spectra reported in Ref. 20), and our theoretical predictions obtained using different values for the pair's confining potential and effective mass. C: $m_{W,hh}=0.59$, $V=266$ meV. G: $m_W,hh=0.341$, $V=316$ meV.

Transition	E_{exp} (eV)	E_G (eV)	E_C (eV)
$0\rightarrow0$	1.1	1.112	1.144
$0\rightarrow1(2)$	1.17	1.176	1.197
$0\rightarrow3$	1.24	1.224	1.236

square-based pyramid with $b=110$ Å and $h=60$ Å. The agreement obtained with parametrization G is very good for all three peak positions, whereas in this particular case, parametrization C only gives a good estimate of the transition energy to the third excited state (since our model predicts the first and second excited hole states to be degenerate, the third peak has been attributed to a transition to the third excited hole level in Table III).

For an InAs pyramidal dot with $b=200$ Å and $h=70$ Å, our calculations, unlike those of Refs. 21,7, and 9 which, as they themselves admitted,[7] are unable to reproduce this feature, predict five different electron states (actually we predict six bound states, the first and second excited states being degenerate in our model, so that there are only five distinct energy levels). The PL spectrum of such a sample grown by Schmidt *et al.*[19] shows five peaks which they attributed to transitions between electron and hole states with the same quantum numbers and therefore are consistent with the existence of five different electronic energy levels in the QD. They also mentioned the existence of the double degeneracy of the first electron and hole excited states, with $m=\pm1$. Moreover, as can be seen in Table IV, the transition energies we predict for such a QD with both parametrizations are in good agreement with the experimental values deduced from the PL spectra. In this particular case, parametrization C seems to be more suitable for the calculation of the ground state recombination energy, whereas parametrization G appears to be more appropriate for excited level transitions. It is worth mentioning, however, that in both the samples used by Schmidt *et al.* the substrate was not rotated during the InAs deposition, allowing the formation of dots with a wide range of sizes and densities. As a result a broadening of the PL peaks is obtained, with a FWHM of the Gaussian best fit to experimental data of about 60 meV. As discussed in the above Sec. IV, this again implies that within this error it is hardly possible to decide which of the two parametrizations used (i.e., which pair $V_{0,hh}$, or $m_{hh,z}$) is the most suitable one for describing this system.

TABLE IV. Transition energies: comparison between experimental values (deduced from PL spectra of Ref. 19), and our theoretical predictions C: $m_{W,hh}=0.59$, $V=266$ meV. G: $m_{W,hh}=0.341$, $V=316$ meV.

Transition	E_{exp} (eV)	E_C (eV)	E_G (eV)
$0\rightarrow0$	1.01	1.017	0.979
$1\rightarrow1$	1.10	1.143	1.112
$2\rightarrow2$	1.17	1.239	1.214
$3\rightarrow3$	1.23	1.262	1.237
$4\rightarrow4$	1.29	1.288	1.264

TABLE V. Transition energies: comparison between experimental values (deduced from PL and PLE spectra of Ref. 24), and our theoretical predictions obtained using different values for the pair confining potential and effective mass. C: $m_{W,hh}=0.59$, $V=266$ meV. G: $m_{W,hh}=0.341$, $V=316$ meV.

Transition	E_C (eV)	E_G (eV)	E_{exp} (eV)
$0\rightarrow0$	1.199	1.168	1.220
$1\rightarrow1$	1.288	1.261	1.270
$2\rightarrow2$	1.306	1.280	1.284
$3\rightarrow3$	1.360	1.338	1.332
$4\rightarrow4$	1.363	1.341	1.340
$5\rightarrow5$	1.398	1.378	1.380
$6\rightarrow6$	/	/	1.412

The calculated energy splittings $\Delta E^{C}_{01,hh}=22$ meV and $\Delta E^{G}_{01,hh}=29$ meV between the ground and first excited heavy-hole states in this structure are also in excellent agreement with the experimentally estimated value of $\Delta E^{exp}_{01,hh}=27$ meV, obtained by combining capacitance and PL measurements.[19] The predicted electron energy splitting $\Delta E_{01,e}$ however, is about two times larger (104 meV) than was determined to be by capacitance[19] and far-infrared[22,15] measurements (i.e., ≈50 meV) on the same or similar samples.

Perhaps, as pointed out by Nishiguchi and Yoh,[23] an energy-dependent effective mass would improve the agreement with the experimental data, reducing the energy-level separation which is overestimated by the usual effective-mass approximation. The constant confining potential approximation, which is the other main assumption our calculations are based on, should not significantly influence the electronic level separation, as its actual value is always almost constant throughout the dot, but is expected to affect the hole level alignment because of the more complex shape of its real profile in structures with an aspect ratio of 1. It should be a better approximation for flatter structures with high aspect ratios, where both the electron and hole confining potentials have almost a square well shape.[10]

In a more recent paper, Noda *et al.*[24] reported six excited level transitions, which they identified as transitions between excited states of electron and holes with the same quantum number. In Table V we present a comparison between their experimental values and our theoretical predictions obtained by using the usual two parametrizations C and G, for the transition energies of a rectangular-based pyramidal QD of height 30 Å and base dimensions 250 and 300 Å along $[110]$ and $[1\bar{1}0]$ directions, respectively. In this case our model predicts the first and second excited levels not to be degenerate, because of the different symmetry of the system (i.e., the pyramid is not square based). It must be mentioned that the transition between the electron and hole states $|100\rangle,|110\rangle$, and $|020\rangle$ (reported in Table V as $1\rightarrow1$, $3\rightarrow3$, and $5\rightarrow5$) do not appear in the PL spectrum as visible peaks, but were identified by Noda *et al.* as hidden peaks by means of a careful comparison between theoretical and ex-

perimental studies of the PL and photoluminescence excitation polarization properties, which permitted the modes of the higher energy levels of the PL spectrum to be assigned. They suggested that the weak emission of these hidden peaks could be due to the strong interaction with phonons, since the energy difference between $|000\rangle$ and $|100\rangle$ in the conduction band is close to twice the InAs LO-phonon energy.

Again parametrization C gives a good estimate for the ground state energy levels, while the values calculated with parametrization G are in excellent agreement with the transition energies between excited states. Our model predicts six bound electron states, thus the absence of any value for the transition between the sixth excited electron and heavy-hole energy levels. However, Noda *et al.* mentioned that this last peak may be due to the wetting layer signal as well.

The sample grown very recently by Murray *et al.*,[25] using a relatively high substrate temperature and a very low growth rate, presents a very small linewidth of only 24 meV, which indicates a small size distribution of the dots, (this has been confirmed by atomic force micrographs that evidenced islands with a mean height of 7 nm and a diameter of 40 nm), and an emission wavelength for the ground-state transition of 1.29 μm (=961 meV), as obtained from a PL spectrum at room temperature. The emission from the first excited state is present around 1.2 μm (=1033 meV). For a square-based pyramid of the same dimensions, our model (parametrization *C*) predicts such transition energies at 962 and 1025 meV, respectively. This is an astonishingly excellent agreement, and means that QD's grown under such conditions are very stable, and their dimensions are not altered significantly by the capping process.

Another spectral position well reproduced by our model is that obtained by Toda *et al.*[26] in near-field magneto-optical spectroscopy measurements of single self-assembled QD's. The structures they investigated have lateral size of ~ 200 Å and height of ~ 20 Å, as indicated by AFM studies of uncapped layers. The typical magnetic-field dependence of the peak energies from a single QD they showed has a value of about 1347 meV for zero magnetic field. The values calculated with our model are 1346 (parameterization *C*) and 1321 meV (parameterization *G*). We calculate only one bound electron state for such structures. It is worth mentioning, however, that the spatially resolved luminescence spectrum reported presents a number of sharp emission lines extending from ~ 1260 to ~ 1350 meV.

We would like to stress that even though our theory is not directly affected by the particular aspect ratio of the dots (because we do not compute the couple confining potential and effective mass for each structure, but rely on the values of more sophisticated treatments given in the literature), the shape of the pyramids nevertheless indirectly influences our results due to the different confining potential and effective mass pairs that have to be chosen for different aspect ratios of the dots. Thus our method for computing energy eigenstates and eigenvalues for pyramidal quantum dots can in principle be applied to any pyramidal structure with any aspect ratio, but the accuracy of the results depends strongly on the particular choice of the confining potentials and strictly related effective masses to be used in the calculations. Nevertheless, the values $m_{W,hh}=0.59$ and $V=266$ meV (parameterization *C*) have proved to reproduce well the ground state energies of all the experimental spectra considered, while the pair $m_{W,hh}=0.341$ and $V=316$ meV (parametrization *G*) gives a good agreement with the transition energies between excited states.

VI. CONCLUSIONS

A single-band, constant-confining-potential model has been applied to self-assembled InAs pyramidal dots in order to determine their electronic structure. By choosing different pair of heavy-hole confining potential and effective masses, the calculated energy eigenvalues and transition energies can be tuned to agree with those derived by means of more sophisticated treatments which take into account features such as the microscopic details of the strain, the mixing between light-hole and heavy-hole bulk bands, and the variation of the confining potential as a function of position inside the dot. The predictions of the model have been compared with several spectra reported in the literature by different authors. Very good agreement with experimental values of the transition energies (deduced from PL spectra) has been found. Furthermore the number of peaks (i.e., transitions between electron and hole states of the same quantum number, as identified by the experimentalists) in such spectra matches the theoretically predicted number of bound states for the considered structure (a feature which other more complex models fail to reproduce) and the hole energy splitting between ground and first excited states deduced from capacitance and PL measurements is in excellent agreement with our calculated values. The model therefore has proved to be suitable not only to predict ground-state eigenenergies but also the number and energy values of the transitions between bound excited states (with the same quantum number). It is postulated that an energy dependence for the effective mass in the Hamiltonian could improve the agreement with the energy separation between ground and first excited electron states.

ACKNOWLEDGMENTS

The authors would like to thank the School of Electronic and Electrical Engineering, the Faculty of Engineering and the University of Leeds for financial support.

[1] I.N. Stranski and L. Von Krastanov, Akad. Wiss. Lit. Mainz Abh. Math. Naturwiss. Kl. **146**, 797 (1939).

[2] D.J. Eaglesham and M. Cerullo, Phys. Rev. Lett. **64**, 1943 (1989).

[3] D. Gershoni, H. Temkin, G.J. Dolan, J. Dunsmuir, S.N.G. Chu, and M.B. Panish, Appl. Phys. Lett. **53**, 995 (1988).

[4] S. Gangopadhyay and B.R. Nag, Nanotechnology **8**, 14 (1997).

[5] E. Anderson, Z. Bai, C. Bischof, J. Demmel, J. Dongarra, J. Du Croz, A. Greenbaum, S. Hammarling, A. McKenney, S. Ostruchov, and D. Sorensen, *LAPACK—Users' Guide* (Society for Industrial and Applied Mathematics, Philadelphia, 1995).

[6] D. Ninno, M.A. Gell, and M. Jaros, J. Phys. C **19**, 3895 (1985).
[7] M.A. Cusack, P.R. Briddon, and M. Jaros, Phys. Rev. B **54**, R2300 (1996).
[8] P. Harrison, Fei Long, and W.E. Hagston, Superlattices Microstruct. **19**, 123 (1996).
[9] M. Grundmann, O. Stier, and D. Bimberg, Phys. Rev. B **52**, 11 969 (1995).
[10] M.A. Cusack, P.R. Briddon, and M. Jaros, Phys. Rev. B **56**, 4047 (1997).
[11] Al.L. Efros and A.L. Efros, Fiz. Tekh. Poluprovodn. **16**, 1209, (1981) [Sov. Phys. Semicond. **16**, 772 (1982)].
[12] M. Grundmann, J. Christen, N.N Ledentsov, J. Böhrer, D. Bimberg, S.S. Ruvimov, P. Werner, U. Richter, U. Gösele, J. Heydenreich, V.M. Ustinov, A.Yu. Egorov, A.E. Zhukov, P.S. Kop'ev, and Zh.I. Alferov, Phys. Rev. Lett. **74**, 4043 (1995).
[13] D. Leonard, K. Pond, and P.M. Petroff, Phys. Rev. B **50**, 11 687 (1994).
[14] J.M. Moison, F. Houzay, F. Barthe, L. Leprince, E. Andre', and O. Vatel, Appl. Phys. Lett. **64**, 196 (1994).
[15] M. Fricke, A. Lorke, J.P. Kotthaus, G. Medeiros-Ribeiro, and P.M. Petroff, Europhys. Lett. **36**, 197 (1996).
[16] S. Sauvage, P. Boucaud, F.H. Julien, J.-M. Gerard, and J.-Y. Marzin, J. Appl. Phys. **82**, 3396 (1997).
[17] Y. Nabetani, T. Ishikawa, S. Noda, and A. Sakai, J. Appl. Phys. **76**, 347 (1994).
[18] R. Murray, S. Malik, P. Siverns, D. Childs, C. Roberts, B. Joyce, and H. Davock, Jpn. J. Appl. Phys. **38**, 496 (1999).
[19] K.H. Schmidt, G. Medeiros-Ribeiro, M. Oestreich, P.M. Petroff, and G.H. Döhler, Phys. Rev. B **54**, 11 346 (1996).
[20] M. Grundmann, N.N. Ledentsov, O. Stier, D. Bimberg, V.M. Ustinov, P.S. Kop'ev, and Zh.I. Alferov, Appl. Phys. Lett. **68**, 979 (1996).
[21] J.Y. Marzin and G. Bastard, Solid State Commun. **92**, 437 (1994).
[22] H. Drexler, D. Leonard, W. Hansen, J.P. Kotthaus, and P.M. Petroff, Phys. Rev. Lett. **73**, 2252 (1994).
[23] N. Nishiguchi and K. Yoh, Jpn. J. Appl. Phys., Part 1 **36**, 3928 (1997).
[24] S. Noda, T. Abe, and M. Tamura, Physica E (Amsterdam) **2**, 643 (1998).
[25] R. Murray, D. Childs, S. Malik, P. Siverns, C. Roberts, J.-M. Hartmann, and P. Stavrinou, Jpn. J. Appl. Phys. **38**, 528 (1999).
[26] Y. Toda, S. Shinomori, K. Suzuki, and Y. Arakawa, Appl. Phys. Lett. **73**, 517 (1998).